Journal of CO2 Utilization 102 (2025) 103225

Contents lists available at ScienceDirect

Journal of CO2 Utilization

journal homepage: www.elsevier.com/locate/jcou

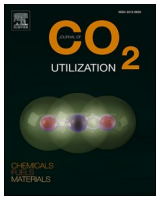

Net-zero sustainable aviation fuel (SAF) production via CO_2 hydrogenation in low-temperature Fischer-Tropsch synthesis: Process design and alternatives

Luis Vaquerizo *, Diego Rego-Fernández

Institute of Bioeconomy, PressTech Group, Department of Chemical Engineering and Environmental Technology, University of Valladolid, Doctor Mergelina s/n, Valladolid 47011, Spain

ARTICLE INFO

Keywords:
Process integration
Optimal process design
Energy efficiency
Dividing-wall column
Steam turbine

ABSTRACT

Sustainable Aviation Fuel (SAF) is fundamental for decarbonizing the aviation sector, which remains one of the hardest industries to electrify. Among the available production routes, SAF derived from indirect CO_2 hydrogenation stands out as a promising alternative, delivering drop-in fuels compatible with existing infrastructure. This work presents and compares three thermally self-sufficient process alternatives for SAF production from captured CO_2, green hydrogen, and renewable electricity. The base case follows a conventional configuration consisting of Reverse Water Gas Shift (RWGS), Fischer-Tropsch (FT), hydrocracker, and Auto-Thermal Reformer (ATR) reactors. The first alternative replaces the ATR with two furnaces and substitutes the PSA-based CO_2 separation with an amine absorption unit. It also includes an isomerization bed to reduce SAF's freezing point, a Dividing Wall Column (DWC) for efficient separation, and a steam turbine to recover part of the plant's power demand. The second alternative retains the ATR while integrating CO_2 capture, the isomerization bed, and the DWC. The analysis shows that maintaining the ATR reactor reduces hydrogen consumption (0.52 kg H_2 per kg of products in the second alternative), being economically more favorable (3.65 €/L of SAF) than minimizing power consumption (716 kWh per ton of products in the first alternative), given the high cost of electrolytic hydrogen. In addition, the DWC proves to be the most efficient separation option, requiring the lowest reboiler duty and the fewest trays. All process configurations produce water as the only byproduct (approximately 3.3 kg H_2O/kg products), and achieve net-negative greenhouse gas emissions of up to −2 kg CO_2eq per kg of product.

1. Introduction

The aviation sector is recognized as one of the most challenging to decarbonize, primarily due to its reliance on energy-dense liquid fuels [1] and the need for alternative fuels that are fully compatible with existing aircraft engines and global fuel infrastructure [2]. Air travel demand continues to rise, with passenger numbers surpassing 4 billion in 2017 [3]. In response, the International Air Transport Association (IATA) has committed to achieving net-zero CO_2 emissions in the aviation sector by 2050 through the adoption of sustainable aviation fuels (SAF) [4]. While SAF can reduce emissions by up to 75 %, current estimates indicate they may cost up to ten times more than conventional jet fuels. This price disparity could lead to flight ticket increases of 100–150 % today, and 40–80 % by 2050, [5], making SAF economically unviable without substantial policy support or significant technological advances [6].

Current sustainable aviation fuel (SAF) production pathways can be broadly categorized into four main families [7]. The first is the Hydroprocessed Esters and Fatty Acids (HEFA) route, which involves hydrogenating fatty acids into hydrocarbons. Second is the Alcohols-to-Jet (ATJ) pathway, where alcohols produced via chemical synthesis or fermentation are converted into hydrocarbons. Third are biomass-based routes, in which biomass is gasified into syngas, liquefied into biooil, or fermented into alcohols or hydrocarbons. Lastly, Fischer-Tropsch (FT) synthesis can be used to convert CO_2 directly into hydrocarbons (direct route) or indirectly via conversion to CO using the Reverse Water Gas Shift (RWGS) reaction (indirect route).

At present, most SAF is produced through the HEFA process. However, this production route is constrained by the limited availability of lipid-rich feedstocks and ongoing concerns over food versus fuel

* Corresponding author.
E-mail address: luis.vaquerizo@uva.es (L. Vaquerizo).

https://doi.org/10.1016/j.jcou.2025.103225
Received 6 July 2025; Received in revised form 4 September 2025; Accepted 13 September 2025

tradeoffs [8]. The ATJ route, particularly with methanol as the primary alcohol, offers the advantage of being thermally self-sufficient due to the exothermic nature of its reactions, thereby reducing thermodynamic losses. Nevertheless, it remains a complex process with relatively low carbon efficiency [2]. Biomass-based pathways face challenges primarily related to feedstock availability, cost, and the high oxygen content of biomass-derived intermediates [9].

Meanwhile, FT synthesis using green hydrogen and captured CO_2 presents two key advantages: it enables the direct utilization of a greenhouse gas and produces a fuel that can be blended with conventional kerosene at up to 50 % without modifications [10]. However, this route still faces significant challenges, particularly in catalyst development, process integration, and the high cost of green hydrogen [11,12]. When comparing the direct and indirect CO_2-to-Fischer-Tropsch conversion routes, the direct hydrogenation of CO_2 into hydrocarbons is a promising approach, as it eliminates the need for a Reverse Water Gas Shift (RWGS) reactor. However, this pathway remains an active area of research and is still technically immature. To date, it has only been demonstrated at the laboratory scale, with no commercial-scale implementations reported [13,14]. Key limitations include low CO_2 conversion rates, poor product selectivity, and rapid catalyst deactivation [15,16]. In contrast, the indirect conversion route, where CO_2 is first converted to CO via the RWGS reaction before undergoing FT synthesis, has reached a higher Technology Readiness Level (TRL) [11]. It is currently considered the most efficient route for SAF production via CO_2 hydrogenation from both energetic and exergetic perspectives [7]. Nevertheless, it is highly energy-intensive, primarily due to the significant hydrogen demand, highlighting the importance of efficient heat integration and optimized plant design [17] prioritizing CO_2 sources with high concentration levels [18].

Given the urgent need for scalable, carbon-neutral aviation fuels and the limitations of current production technologies, advancing the technical understanding and performance of SAF production pathways is essential [16]. Among existing options, the HEFA route is constrained by limited feedstock availability; the methanol-based route is process-intensive and offers lower carbon efficiency; biomass routes face challenges related to feedstock supply and the formation of oxygenated compounds; and the direct CO_2 conversion route remains technically immature. This study focuses on the indirect CO_2-to-FT route, a high-TRL alternative, using rigorous Aspen Plus simulations. To our knowledge, this is the first work to evaluate, within a complete process simulation, whether it is more advantageous to maintain the ATR reactor, thereby reducing hydrogen consumption, or to replace it with a combination of two furnaces and a steam turbine, which lowers overall energy consumption. We also present the first explicit inclusion of an isomerization bed after the hydrocracking bed in SAF simulations, demonstrating its critical role in meeting the required freezing point of SAF. Furthermore, we provide the first comparative assessment of advanced separation sequences for SAF production, analyzing a stripper combined with a distillation column, a distillation column with a pumparound and a side stripper, and a dividing-wall column (DWC), and showing how each configuration and its operating parameters affect both process efficiency and product quality. The findings support more efficient design and optimization of FT production plants based on the indirect CO_2 pathway and enable more robust comparisons with other SAF production technologies.

2. Problem statement and objectives

The indirect CO_2-to-Fischer Tropsch SAF production route is a high-TRL pathway for generating SAF that can be directly blended (up to 50 %) with conventional fossil-derived kerosene. Despite its advanced technological maturity, the process remains complex, involving at least three major reactor units: a reverse water gas shift (RWGS) reactor, a Fischer-Tropsch reactor, and a hydrocracker. The main drawback of this route, compared to alternative SAF production pathways, lies in the need to convert CO_2 into CO in the RWGS reactor, a reaction that requires very high operating temperatures (900–950ºC) and significant energy input [19]. Additionally, the syngas produced in this step must be purified to remove the unreacted CO_2, which is then recycled upstream to the RWGS reactor. Meeting the official SAF specifications also presents challenges. Certain properties, such as the freezing point, require the integration of additional units, such as an isomerization reactor, to ensure compliance. Furthermore, the design and optimization of the separation system is not trivial, as the distillation columns must be carefully configured and operated to meet product specifications.

To assess and improve the performance of this SAF production pathway, this work has reviewed the existing literature on indirect CO_2-to-SAF via indirect Fischer-Tropsch synthesis and proposes redesign processes to meet the following objectives:

1. Evaluate the use of an amine absorption unit for syngas purification: investigate whether amine absorption can effectively remove CO_2 from the RWGS syngas stream. Key design parameters, such as the number of stages in the absorption and regeneration columns, amine flowrate, and reboiler duty, are quantified. This approach has been successfully applied in similar CO_2 capture processes [20–22].
2. Incorporate an isomerization reactor: add an isomerization unit to convert the predominantly linear paraffins produced in the FT reactor [23] into branched paraffins, which possess lower freezing points. As previous studies have shown, SAF composed solely of linear paraffins fails to meet freezing point requirements [24].
3. Optimize the separation sequence: explore alternatives to the conventional separation system, typically involving a stripper and a second distillation column. Two configurations are analyzed:

- A single distillation column with a pumparound and a lateral stripper, inspired by conventional refinery practice (crude distillation units, hydrocrackers, delayed cokers).
- A dividing wall column (DWC): an intensified alternative that has proven effectiveness in similar processes such as CO_2-to-methanol and CO_2-to-DME [25,26].

4. Perform a heat integration study via pinch analysis: assess heat flows throughout the process to determine whether it is thermally self-sufficient or requires external heat input. In particular, the impact of the amine absorption unit and its reboiler duty is evaluated.

This work presents the simulation results for two redesigned process alternatives for a 225 ktpy SAF production plant. This production capacity corresponds to the full refueling of 10,771 Boeing 737 aircraft per year [27], which is equivalent to the operating capacity of a medium-sized airport [28]. Both alternatives are benchmarked against the base case proposed by Atsonios et al. (2023) [7] for the indirect CO_2-to-SAF FT route.

- Alternative 1 includes an amine absorption unit and an isomerization reactor but replaces the ATR with a pair of furnaces to supply heat to the RWGS and hydrocracker reactors. Additionally, it integrates a steam turbine to partially cover the electricity demand of the process.
- Alternative 2 also incorporates an amine absorption unit for syngas purification, an isomerization reactor downstream of the hydrocracker to produce branched paraffins, and an optimized autothermal reformer (ATR) that supplies high-temperature heat to the RWGS reactor while simultaneously generating hydrogen, which is recycled upstream.

By comparing these three configurations, this study provides insight into the impact of different design choices on overall process performance, aiding in the development of an optimized SAF production route.

3. Simulation approach

A 225 ktpy SAF production plant has been simulated in this work. In both alternatives, SAF and diesel productions are maximized by setting the SAF flash point to 38ºC and the diesel distillation temperature for 95 % volumetric recovery to 360ºC, in accordance with SAF (ASTM D7566 Annex 1) and diesel (ASTM-D975 2D) specifications. While the required CO_2 flowrate is modified to obtain the desired SAF production rate, hydrogen consumption is treated as a dependent variable and automatically adjusted to satisfy the reagents ratios in the different reactors of the plant.

3.1. Property model

The two alternatives presented in this work, along with the base case scenario of Atsonios et al., 2023 [7] have been simulated using Aspen Plus® v14.0. The Peng-Robinson Equation of State (PR-EOS) with the Boston-Mathias (BM) modification has been selected as thermodynamic package due to the apolar nature of the compounds and the high operating pressures (up to 35 bar). Steam tables have been used as free water method. For the simulation of the amine absorption unit, the Electrolytes Non-Random-Two-Liquid (ELECNRTL) method has been selected. This is an extension of the NRTL method designed for electrolytes modeling at both low and high concentrations. The ELECNRTL package uses the Redlich-Kwong Equation of State (RKEOS) to model the vapor phase, which is appropriate for the low operating pressure of this unit (up to 4 bar).

3.2. Product specifications

Fischer-Tropsch hydroprocessed synthesized paraffinic SAF and diesel specifications are governed by the international codes ASTM D7566 Annex 1 and ASTM-D975 2D. However, the diesel produced also meets the more stringent EURO V Fuel Quality Directive. While most specification values (flash point, cetane number, density, distillation temperature) are directly calculated by Aspen Plus, the freezing point of kerosene has been obtained using a blending index-based method [29].

3.3. Reactor modeling

Five different reactors are included in the simulations. The only difference between Alternative 1 and Alternative 2 is the fact that, in the second alternative, the autothermal reformer is excluded. Table 1 summarizes the modeling strategies applied to each reactor, which are described below for clarity:

- Reverse water gas shift reactor (RWGS reactor):
  The RWGS reactor converts CO_2 into CO via hydrogenation, with methanation (Sabatier reaction) occurring as an undesired reaction. Given the high reaction temperature (900ºC), the reactions are assumed to reach equilibrium. Therefore, the reactor has been modeled using the RGIBBS reactor type in Aspen Plus. A H_2/CO_2 ratio of 2 is applied, in line with previous studies [7]. The main reactions are:

$$CO_2 + H_2 \leftrightarrows CO + H_2O \quad (1)$$

$$CO_2 + 4H_2 \leftrightarrows CH_4 + 2H_2O \quad (2)$$

- Fischer-Tropsch reactor (FT reactor):
  The FT reactor converts syngas ($CO+H_2$) into linear paraffins [24]. For hydrocarbons with more than four carbon atoms, the selectivity follows an Anderson-Schulz-Flory (ASF) distribution, considering a chain growth probability factor (α) of 0.92 based on a cobalt catalyst under the selected operating conditions. Both the value of α and the selectivities for lighter hydrocarbons are provided in the work of Adams and Barton. 2011 [30]. The operating conditions are fixed at 240ºC and 35 bar, with a H_2/CO ratio of 2 [7]. The reactor is modeled

Table 1
Reactor models used to simulate Alternatives 1 and 2.

Reactor	Reactor Model	Operating Conditions	Reactions	Conversion	Reference
Reverse Water Gas Shift	RGIBBS	900ºC / 5 bar H_2/CO_2 = 2 (mol)	$CO_2 + H_2 \leftrightarrows CO + H_2O$ $CO_2 + 4H_2 \leftrightarrows CH_4 + 2H_2O$	Gibbs Free Energy Minimization	Atsonios et al., 2023 [7]
Fischer-Tropsch	RSTOIC	240ºC / 35 bar H_2/CO = 2 (mol)	$nCO + (2n+1)H_2 \rightarrow C_nH_{2n+2} + nH_2O$ $CO + H_2O \rightarrow CO_2 + H_2$ Light gases selectivities: CH_4: 0.05, C_2H_4: 0.0005, C_2H_6: 0.01, C_3H_6: 0.02, C_3H_8: 0.01, C_4H_8: 0.02, C_4H_{10}: 0.01, CO_2: 0.01	C1 to C64; CO: 0.85 ASF Distribution, α: 0.92	Atsonios et al., 2023 [7] Meurer and King, 2021 [24] Adams and Barton, 2011 [30]
Hydrocracker	RSTOIC	Tin: 325ºC, Pin: 35 bar Adiabatic H_2: Stoichiometric	$C_nH_{2n+2} + H_2 \rightarrow 2C_n/2H_{n+2}$ $CnH_{2n+2} + H_2 \rightarrow C_{(n-1)/2}H_{n-1} + C_{(n+1)/2}H_{n+3}$	C16 to C64; X = 0.96	Gamba et al., 2010 [37]
Isomerization	RSTOIC	Hydrocracker Outlet, Adiabatic	$C_nH_{2n+2} \rightarrow C_nH_{2n+2}$ (isomer)	C6 to C22 C6: 0.7407, C7: 0.6215 C8: 0.5619, C9: 0.5216 C10: 0.5201, C11: 0.5425 C12: 0.5723, C13: 0.6408 C14: 0.69, C15: 0.7437 C16: 0.7958, C17: 0.8405 C18: 0.8554, C19: 0.9195 C20: 0.9225, C21: 0.9195 C22: 0.9359	Gamba et al., 2010 [37]
Autothermal Reactor	RGIBBS	950ºC / 5 bar O_2/C: 0.478 H_2O/C: 0.2	$2CH_4 + O_2 + CO_2 \leftrightarrows 3H_2 + 3CO + H_2O$ $4CH_4 + O_2 + 2H_2O \leftrightarrows 10H_2 + 4CO$	Gibbs Free Energy Minimization	Atsonios et al., 2023 [7]

as a stoichiometric reactor (RSTOIC) governed by the paraffinic production reaction and a secondary water gas shift reaction:

$$nCO + (2n+1)H_2 \rightarrow C_nH_{2n+2} + nH_2O \quad (3)$$

$$CO + H_2O \rightarrow CO_2 + H_2 \quad (4)$$

In this work, a cobalt-based (Co) catalyst was selected because of its superior selectivity toward paraffins in the SAF range, its higher stability compared with iron-based (Fe) catalysts, and its significantly lower cost relative to ruthenium-based (Ru) catalysts [31]. Cobalt catalysts are known to deactivate primarily through wax deposition rather than by oxidation, sintering, or coking [32]. The Fischer–Tropsch reactor is assumed to be a multitubular fixed-bed reactor, consistent with industrial practice [33]. In such configurations, pressure drops typically range from 0.02 to 0.15 bar/m, depending on catalyst type, loading, and surface velocity [34]. The operating conditions considered in this study reflect the LTFT regime, with pressures between 20 and 35 bar and CO partial pressures of 5–15 bar. These conditions enhance C_5^+ hydrocarbon yields, minimize methane formation, and enable hydrogen conversions of up to 90 % [35]. Regarding feedstock purity, previous studies indicate that, for cobalt catalysts, CO_2 can be tolerated as an inert up to concentrations of approximately 10 % mol without significantly impacting activity or selectivity [36]. Nonetheless, in this work, it is assumed that the CO_2 content is reduced to the ppm level via an amine absorption unit to maximize the effective partial pressures of H_2 and CO in the feed.

We acknowledge that using a stoichiometric reactor model to represent the FT reactor does not fully capture the effects of catalyst behavior, variations in operating conditions, changes in reagent partial pressures, or the presence of impurities. These factors can indeed influence process performance. A more detailed kinetic-based reactor model would be necessary to account for such effects if catalyst formulation or operating conditions diverge from those considered in this study.

– Hydrocracker:

The hydrocracker reactor breaks the long-chain hydrocarbons into shorter ones within the kerosene and diesel range. The operating conditions (325ºC, 35 bar), hydrogen content (stoichiometric), and conversion (96 % for C_{16}-C_{64} hydrocarbons) are based on the work of Gamba et al., 2010 [37], who studied hydrocracking and isomerization of a Fischer-Tropsch wax. The reactor is modeled as a stoichiometric reactor (RSTOIC) using two reactions, depending on whether the number of carbons of the initial paraffin is even or odd:

$$C_nH_{2n+2} + H_2 \rightarrow 2C_{n/2}H_{n+2} \quad (5)$$

$$C_nH_{2n+2} + H_2 \rightarrow C_{(n-1)/2}H_{n-1} + C_{(n+1)/2}H_{n+3} \quad (6)$$

– Isomerization reactor

Although represented as a separate unit in the simulation, the isomerization reactor is, in reality, the final catalytic bed within the hydrocracking reactor. It operates under the outlet conditions of the hydrocracker, converting linear paraffins into branched ones, which have a lower freezing point. The conversion data is again taken from Gamba et al. (2010) [37]. It is modeled as an RSTOIC reactor with the simplified reaction:

$$C_nH_{2n+2} \rightarrow C_nH_{2n+2} \text{ (isomer)} \quad (7)$$

– Autothermal reformer (ATR):

The ATR converts methane and light hydrocarbons produced in the FT reactor into syngas (CO + H_2) while generating a significant high-temperature heat. In this work, the operating conditions (950ºC, 5 bar) have been selected in line with previous works [7]·H_2O/C and O_2/C ratios have been optimized to maximize syngas production while maintaining the thermal self-sufficiency of the process. Due to the high reaction temperature, the reactions are assumed to reach equilibrium and are modeled with an RGIBBS reactor. The two main reactions, assuming methane as the reference hydrocarbon, are:

$$2CH_4 + O_2 + CO_2 \leftrightarrows 3H_2 + 3CO + H_2O \quad (8)$$

$$4CH_4 + O_2 + 2\,H_2O \leftrightarrows 10H_2 + 4CO \quad (9)$$

3.4. Amine absorption unit modeling

Both the absorber and the regenerator columns of the amine absorption unit have been simulated using the "Rate-Based" approach, a rigorous method that accounts for the mass and heat transfer processes occurring within the column. Flexipac® HC® packing from Koch-Glitsch® has been selected in both columns. This structured metal packing offers a combination of high capacity and low pressure drop [38]. While the bed length influences the CO_2 content in the outlet gas, the column diameter is adjusted according to hydraulic considerations to prevent flooding or weeping issues.

4. Description of alternatives

Two alternatives to the indirect CO_2-to-FT process presented by Atsonios et al., 2023 [7], which serves as the base case scenario, have been simulated and benchmarked against this reference case. Fig. 1 presents the block diagrams of each alternative. To support a better understanding of the alternatives, detailed process flow diagrams and heat and material balances are provided in the Supplementary Information file. Both alternatives are described in detail below:

4.1. Alternative 1

Alternative 1 differs from the indirect CO_2-to-FT process described by Atsonios et al., 2023 [7] in several key aspects. First, it replaces the pressure swing adsorption (PSA) located after the RWGS reactor (PSA-1) with an amine absorption unit for CO_2 recovery. It also omits the second PSA unit (PSA-2), originally used to recover hydrogen from the FT gas. Instead, this alternative includes a recycling stream that recirculates part of the unreacted gases from the FT reactor. Furthermore, the Auto Thermal Reformer (ATR) is substituted by two furnaces, and the hydrocracker operates under slightly different conditions, incorporating an isomerization bed. A steam turbine is added to cover part of the power consumption in the plant using excess heat from the furnaces. Finally, the two distillation columns are replaced with a single dividing wall column (DWC).

In this configuration, fresh, pure CO_2 is combined with recovered CO_2 from the amine absorption unit and with the flue gas stream exiting the furnaces (after cooling and condensation). The resulting mixture is fed to a two-stage CO_2 compressor (CO2COMP) with intercooling to 55°C. This temperature is selected assuming air is used as the cooling fluid. If cooling water or colder air is available, the intercooling temperature, and thus the compressor power, would decrease. The number of stages in all compressors is fixed to prevent the stage discharge temperature from exceeding 176°C, chosen as the maximum allowable temperature (MAT) [39].

The pressurized CO_2 stream (5 bar) is mixed with hydrogen compressed by the H_2 compressor (H2COMP), also a two-stage unit with intercooling to 55°C. Hydrogen used in the process comes from an electrolyzer and is considered to be saturated with water. The compressed hydrogen is split into three fractions: one part is mixed with the CO_2 stream and sent to the RWGS unit, another part is directed to the FT reactor, and the remainder fraction is sent to the hydrocracker. The combined CO_2 and H_2 stream (with an H_2/CO_2 ratio of 2) enters the RWGS-FEHE, where it is heated to 582°C while simultaneously cooling the RWGS effluent to 480°C.

The RWGS reactor operates at 900°C in a furnace-type configuration,

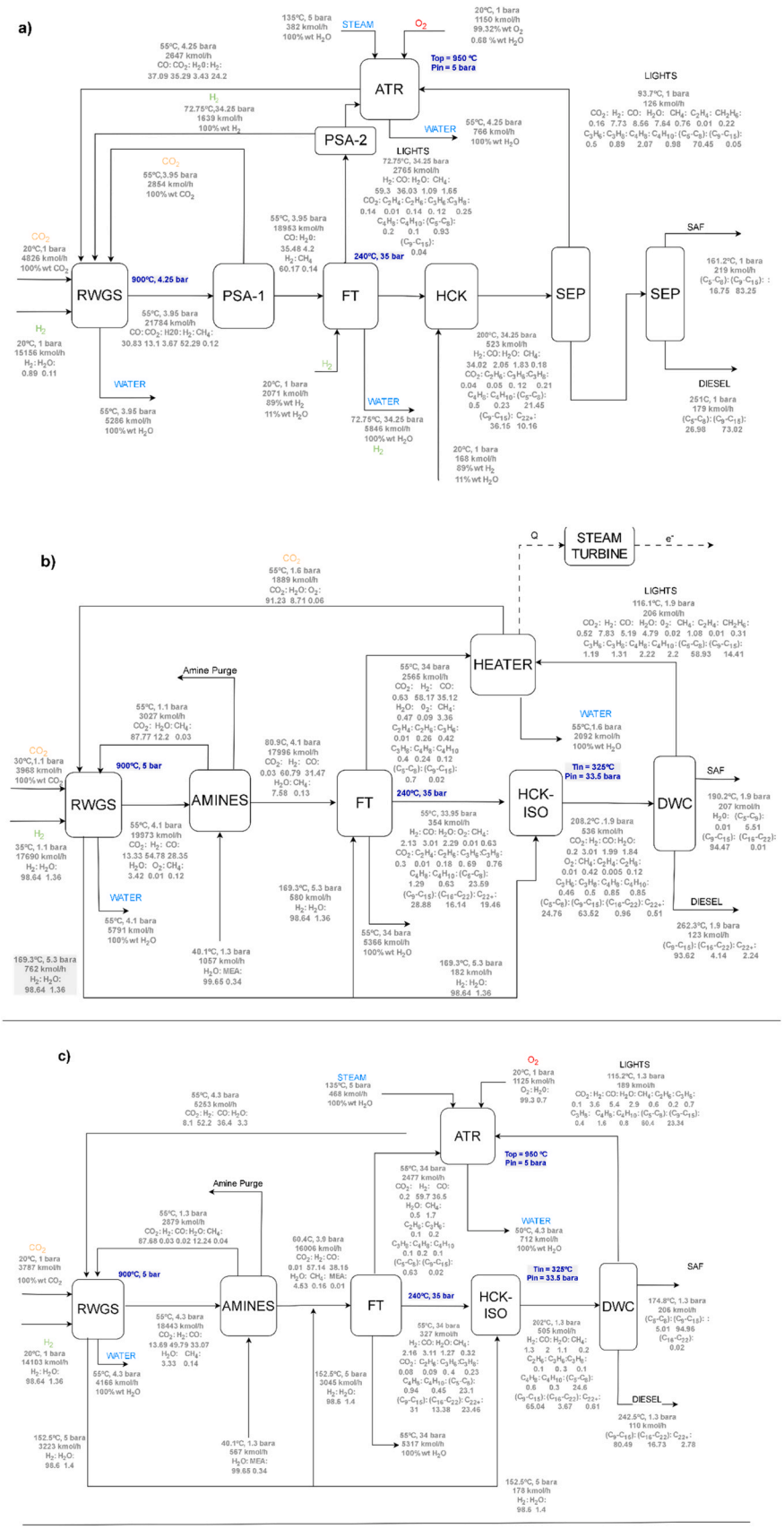

Fig. 1. Block diagrams of the proposed alternatives. a) Original process developed by Atsonios et al. 2023 [7], b) Alternative 1, c) Alternative 2.

achieving a CO_2 conversion of 68.1 %. Some of the heat generated in the RWGS furnace is used to vaporize and superheat boiler feed water (BFW) for the steam turbine and the DWC reboiler. The flue gas from this furnace is mixed with that from the hydrocracker furnace and cooled in an air cooler (FL-COOLER) to 55°C. The resulting two-phase stream is separated in the flue gas separator (FL-SEP) where the aqueous phase is removed, while the gas phase (mainly CO_2) is recycled to the CO_2 compressor.

Saturated oxygen from the electrolyzer is used as the comburent in both the RWGS and hydrocracker furnaces. The oxygen is pressurized to 2 bar using the O_2 compressor (O2COMP) to overcome pressure drops. In both furnaces, a slight excess of oxygen above the stoichiometric requirement is supplied.

After exiting the FEHE, the RWGS reactor product is used to preheat high pressure BFW in heat exchanger RWGS-E1 and then cooled to 55°C in RWGS-E2. Condensed water is removed in the RWGS-SEP, and the remaining gas stream is treated in the amine absorption unit for CO_2 removal. This unit includes a 30-meter absorber operating at 4 bar and a 30-meter regenerator operating at 1.3 bar. A 25 %wt monoethanolamine (MEA) solution is used, with the main operating parameters for CO_2 capture remaining in typical ranges [40]: acid gas loading of 0.38 molCO_2/molAmine and a reboiler duty of 1936 BTU/gal lean solution. The resulting syngas contains 270 ppm of CO_2, and 99.8 % of the CO_2 is recovered at the regenerator outlet and recycled to the CO_2 compressor.

The purified syngas is mixed with fresh hydrogen from the H2COMP to achieve a H_2/CO ratio of 2 at the FT reactor inlet. This mixture is compressed to 35 bar in the FT gas compressor (FT-COMP), a three-stage unit with intercooling to 55°C. The pressurized stream is combined with recycled unreacted gas from the FT reactor and passed through a feed-effluent heat exchanger (FT-FEHE), where it is preheated before entering the FT reactor (FT-REACTOR). In this reactor, hydrocarbons and water are produced by direct reaction of CO and H_2, achieving a CO conversion of 85.2 % [7,24,30].

After cooling in an air cooler (FT-COOLER) to 55°C, the reaction mixture enters the FT separation vessel (FT-SEP). In this vessel, the aqueous phase is removed, and the liquid hydrocarbons are directed to the hydrocracking section. Light gases are either recycled to the FT reactor inlet using the recycling compressor (FT-RCOMP) or sent to the furnaces. In this alternative, 55 % (mol/mol) of the light gas stream is recycled. The split ratio is based on two considerations: maintaining methane in the recycle stream below 4 % mol/mol [41], and managing the trade-off between furnace duty and hydrogen consumption.

The liquid hydrocarbons from FT-SEP are hydrocracked into SAF and diesel-range products. Hydrogen for the hydrocracker is compressed by a booster compressor (H2BOOST) to 35 bar, the reactor's operating pressure. This two-stage unit also includes intercooling to 55°C and provides a stoichiometric amount of hydrogen. After preheating in the hydrocracker FEHE (HCK-FEHE), the stream enters the hydrocracker reactor (HCK-REACTOR), which operates at 325°C and 35 bar. Long-chain hydrocarbons are converted into shorter molecules suitable for SAF and diesel. Immediately after, an isomerization bed transforms linear paraffins into branched paraffins to lower the freezing point. Conversion values are based on Gamba et al. (2010) [37].

Heat from the hydrocracker furnace is also used to generate high-pressure steam for the plant's steam turbine. After cooling in the FEHE, the product is sent to a 20-stage dividing wall column (DWC), operated at 1.3 bar with a 45 % liquid split to the prefractionator. This column separates the stream into three products: a fuel gas (top), which is mixed with FT light gases and used as furnace fuel, SAF (main product), recovered from tray 14, and diesel, collected at the bottom.

The final section of the process is the steam turbine system, which provides part of the electricity needed by the plant. It includes a BFW surge vessel (BFW-SURGE), a high-pressure pump (BFW-PUMP), the vaporizers and superheaters (RWGS-E1 and both furnaces), the steam turbine (STEAM-TURBINE), and the low pressure steam condenser (STEAM-COND). The turbine design is based on the Siemens SST-400 model [42], as its power output (65 MW) aligns with the plant's production.

4.2. Alternative 2

Alternative 2 differs from Alternative 1 in that it retains the Autothermal Reformer (ATR) in the process. As a result, there is no need for a hydrocracker furnace, the heat duty required by the RWGS reactor is fully supplied by the ATR, and a steam turbine is not included. Furthermore, this configuration does not incorporate a recycling compressor after the FT reactor, meaning all light gases produced in the FT section are directed to the ATR. All other modifications relative to the base case scenario of Atsonios et al. (2023) [7] are preserved.

In this configuration, fresh CO_2, CO_2 recycled from the amine absorption unit, and the gas stream from the ATR are combined and pressurized in the CO_2 compressor (CO2COMP), a two-stage unit with intercooling to 55ºC, as in Alternative 1. The pressurized CO_2 stream (5.3 bar) is then mixed with fresh hydrogen supplied by the hydrogen compressor (H2COMP), also a two-stage, 55ºC-intercooled compressor which supplies hydrogen to the RWGS, FT, and hydrocracking sections. As in Alternative 1, saturated hydrogen coming from an electrolyzer is used in the plant.

The resulting gas mixture, with an H_2/CO_2 molar ratio of 2, is sent to the RWGS-FEHE and subsequently to the RWGS reactor (RWGS-REACTOR), where 62.5 % of the CO_2 is converted. After passing through the RWGS-FEHE, the reactor effluent is cooled to 55ºC in an air cooler, and the aqueous phase is separated in the RWGS separator (RWGS-SEP).

As in Alternative 1, unreacted CO_2 is removed from the syngas in an amine absorption unit using a 25 wt% monoethanolamine (MEA) solution. The system consists of a 30 m absorption column operating at 4 bar and a 30 m desorption column at 1.3 bar. The operating parameters of the unit are similar to those of Alternative 1, with an acid gas pickup rate of 0.35 mol CO_2/mol amine and a reboiler heat duty of 1802 BTU/gal lean solution. The treated syngas contains just 80 ppm CO_2, with 99.95 % of the CO_2 recovered at the top of the regenerator and recycled to the CO2COMP.

The clean syngas is then mixed with hydrogen (adjusted to an H_2/CO ratio of 2) and compressed in the FT compressor (FT-COMP), a two-stage, 55ºC-intercooled unit that raises the pressure to 35 bar, the FT reactor's operating pressure. After heating in the FT-FEHE, the feed enters the FT reactor, where 85.2 % of the CO is converted to hydrocarbons. The reactor effluent is cooled first in the FT-FEHE and then in an air cooler (FT-COOLER) to 55ºC. At this temperature, three phases are formed and separated in the FT separator (FT-SEP): an aqueous phase removed from the system, a liquid hydrocarbon phase sent to the hydrocracker, and light gaseous hydrocarbons directed to the ATR section.

The light gases are preheated in the ATR-FEHE, mixed with the overhead stream from the dividing wall column (DWC), and then fed into the ATR reactor (ATR-REACTOR). Here, they react with steam and oxygen at O_2/C and H_2O/C ratios of 0.48 and 0.2, respectively, to prevent coking, maximize hydrogen production, and meet the heat duty requirements of the RWGS reactor. The integration of the ATR and RWGS reactors in a shared furnace-type reactor is proposed to enhance heat recovery. As in Alternative 1, saturated oxygen is compressed in a two-stage, 55ºC-intercooled O_2 compressor (O2COMP) to 5 bar for ATR operation.

The ATR reactor effluent is split into two streams: 60 % (mol) is recycled through the ATR-FEHE, while the remaining portion is directed to the hydrocracker heater (HCK-HEAT). After cooling, the streams are mixed, further cooled in the ATR-COOLER to 55ºC, and sent to a vessel (ATR-SEP) to separate condensed water. The remaining gas is recycled to the CO_2 compressor.

The liquid hydrocarbons recovered in the FT-SEP are mixed with hydrogen, pressurized in the hydrogen booster compressor (H2BOOST), a two-stage, 55ºC-intercooled unit supplied by H2COMP. The resulting stoichiometric mixture, pressurized to 35 bar, is heated in the

hydrocracker FEHE (HCK-FEHE) and then in the HCK-HEAT before entering the hydrocracker reactor (HCK-ISO-REACTOR). This reactor includes a final isomerization bed to convert linear paraffins into branched isomers with lower freezing points. Conversion data is taken from Gamba et al. (2019) [37].

After cooling in the HCK-FEHE, the hydrocracked stream is directed to the DWC, a 23-stage column operating at 1.3 bar, with an internal liquid split ratio of 40 % mol/mol to the prefractionator. The DWC produces SAF (recovered at the 17th tray), diesel (bottoms product), and light gaseous hydrocarbons (top product). The overhead stream is cooled to 55ºC in the FG-COOLER, resulting in a vapor-liquid mixture. These are separated in a vessel and individually pressurized: the liquid in the STGL-PUMP and the gas in the STGL-COMP, both to 5 bar, before being recycled to the ATR section.

5. Results and discussion

5.1. Separation alternatives

The original work by Atsonios et al. (2023) [7] proposed a downstream separation sequence consisting of a stripper followed by a distillation column. In this configuration, the stripper removes light hydrocarbons, while the distillation column separates the stripper's bottoms stream into a sustainable aviation fuel (SAF) cut and a diesel cut. This sequence is effective: the SAF flash point can be tuned by adjusting the stripper's distillate-to-feed ratio, and the diesel T95 temperature can be regulated via the distillation column's reboiler duty. However, this study evaluates for the first time, in the context of SAF production, two alternative configurations: a single distillation column equipped with a pumparound and a lateral stripper, and a dividing wall column (DWC). The analysis is based on the feed stream to the DWC from Alternative 2 (stream HCK-3). Results are summarized in Table 4, and schematics of the three configurations are provided in the Supplementary Information. Optimization of feed location, tray numbers, and extraction points for each configuration follows the methodology detailed in our previous works [25,26].

The strategy followed for adjusting each separation configuration is the maximization of SAF and diesel yields, while ensuring that all relevant specifications are met. Specifically, the SAF flash point is fixed at 38ºC, the minimum value required by ASTM D7566 Annex 1, and the diesel T95 distillation temperature is set to 360ºC, the maximum limit according to the EURO V Directive. Additionally, the SAF-diesel gap is maintained within the −5–10 ºC range, a common industrial practice [43]. With these conditions in place, all other product properties remain within acceptable limits.

As shown in Table 4, all three configurations yield identical product specifications and product distributions, allowing for a direct comparison based on the total number of trays and reboiler duties. The original configuration, consisting of a stripper and a distillation column, requires a total of 34 trays (11 in the stripper and 23 in the distillation column) and a reboiler duty of 5778 kW. The second configuration, which uses a distillation column with a pumparound and a lateral stripper, reduces the total number of trays to 27 (25 in the main column and 2 in the lateral stripper), with a reboiler duty of 3731 kW. The DWC alternative shows the best performance, requiring only 23 trays and a reboiler duty of 2572 kW.

From a design perspective, the DWC alternative is preferred. Nevertheless, some guidelines and strategies to maintain product specifications in each configuration are provided:

- Stripper + Distillation Column: The stripper primarily governs the SAF flash point. If the flash point is too low, the distillate-to-feed ratio should be increased to remove more light compounds. Alternatively, higher reflux and boilup ratios may be applied to improve separation efficiency. The second distillation column controls both SAF and diesel yields and qualities. A lower diesel yield typically results in a heavier product, with an upper constraint defined by the T95 limit (360ºC). The SAF-diesel gap is controlled by adjusting the reflux and boilup ratios, which also directly affect reboiler and condenser duties.
- Distillation Column + Pumparound + Lateral Stripper: As in the previous column, the SAF and diesel cuts are governed by the same principles. The feed enters at tray 18; the pumparound is drawn off at tray 17 and returned at tray 16, while the SAF is extracted from tray 14. The pumparound is used to enhance the separation between the SAF and diesel cuts. A higher pumparound duty improves this fractionation and increases the SAF-diesel gap, while reducing the freezing and flash points of SAF by minimizing diesel entrainment. In this case, the pumparound stream is cooled via an air cooler, but thermal integration could be implemented to recover heat. The lateral stripper's reboiler controls the SAF flash point: increasing its duty removes more light compounds, resulting in a higher flash point. The overall reflux ratio influences separation in the upper part of the column, improving the naphtha-SAF gap. However, a high reflux ratio not matched by an increase in the boilup ratio may condense light compounds into the SAF cut, reducing its flash and freezing points.
- Dividing Wall Column: The operation of a dividing wall column may be more complex because of the challenge of controlling the internal liquid and vapor split ratios [44]. As before, the yields and distillate ranges of SAF and diesel are determined by the extraction rates. Increasing reflux improves the removal of lighter components, resulting in SAF with lower flash and freezing points, while increasing boilup enhances the vaporization of heavier compounds into the SAF cut, raising these values. The internal liquid and vapor split fractions play a critical role in determining the SAF-diesel gap, the SAF flash point, and the reboiler and condenser duties, with non-optimal values meaning worse separation efficiency and higher energy demand.

Considering that this process does not require the operational flexibility typically needed in a conventional refinery, which must accommodate variable crude feeds, the DWC alternative emerges as the most attractive option. It requires only a single column and meets product specifications with the lowest number of trays and reboiler duty.

5.2. Key performance indicators (KPIs)

A comparative analysis of the key performance indicators (KPIs) for the three process configurations, Atsonios et al. (2023), Alternative 1, and Alternative 2, is presented in Table 2. As described in the previous section, all distillation columns have been adjusted to maximize SAF and diesel production while meeting the required product specifications, as detailed in Table 3. In the original process configuration, in line with previous works on SAF production [7,14,19,21], no isomerization bed is included, making it impossible to achieve the required freezing point for SAF (−47ºC) without exceeding the maximum allowable flash point (38ºC). As shown in Table 2, the CO_2 conversions in the RWGS reactor are similar across all three configurations, although slightly higher in Alternative 1 due to a lower concentration of CO and H_2O in the feed stream.

In terms of SAF and diesel production rates, both Alternatives 1 and 2 yield a greater amount of SAF than the original configuration. This difference is attributed to the complete conversion (100 %) of long-chain hydrocarbons to shorter-chain compounds in the hydrocracker of the original process, resulting in lighter distillates with lower flash points. Regarding water production, this parameter is strongly influenced by hydrogen and oxygen consumption. In Alternative 1, part of the light gases produced in the FT reactor are used for heat and power generation. These gases contain hydrogen, which is combusted in the RWGS and hydrocracker furnaces, thereby increasing oxygen demand as a comburent. Although this enhances heat recovery and allows for

Table 2
Key Performance Indicators (KPIs) of the proposed alternatives.

	Atsonios (2023)	This Work-No ATR	This Work-Optimized
SAF Production Rate (kton/y)	225	225	269
Purge to Feed Ratio (mol/mol)	0	0	0
H_2:CO_2 ratio (RWGS reactor inlet) (mol/mol)	2.0	2.0	2.0
H_2:CO ratio (FT reactor inlet) (mol/mol)	2.0	2.0	2.0
CO_2 conversion (RWGS, per pass) (%)	66.9	68.1	62.5
CO conversion (FT, per pass) (%)	85.0	85.2	85.0
SAF yield (overall process) ($kgSAF/kgCO_2$)	0.147	0.179	0.188
Diesel yield (overall process) ($kgDiesel/kgCO_2$)	0.175	0.144	0.135
Water production (overall process) ($kgwat/kgCO_2$)	1.0	1.4	1.1
Power consumption (per ton of SAF & diesel) (kWh/ton)	1274	1710	1697
Power production (per ton of SAF & diesel) (kWh/ton)	0	995	0
Net power consumption (per ton of SAF & diesel) (kWh/ton)	1274	716	1697
External heat (per ton of SAF & diesel) (kW/ton)	0	0	0
External cooling (per ton of SAF & diesel) (kW/ton)	4477	11942	8862
CO_2 utilization (pero unit of SAF & Diesel) (kg/kg)	3.1	3.1	3.1
H_2 consumption (per unit of SAF & Diesel) (kg/kg)	0.51	0.62	0.52
O_2 consumption (per unit of SAF & Diesel) (kg/kg)	0.53	1.48	0.67

Table 3
Products specifications in the proposed alternatives.

	Spec	Atsonios 2023	No ATR (Alternative 1)	Optimized (Alternative 2)
SAF				
Flash Point (°C)	38, min	38	38	38
Freezing Point (°C)	−47, max	−27.8	−55.9	−57
ASTM D86, 10 % v/v (°C)	205, max	154	154	154
ASTM D86, FBP (°C)	300, max	221	228	222
Density at 15°C (kg/m^3)	730–770	737	775	751
Diesel				
Flash Point (°C)	55, min	92.4	83.1	82
ASTM D86, 95 % v/v (°C)	360, max	322	360	360
Density at 15°C (kg/m^3)	845, max	764	786	778
Cetane number	51, min	94.2	70.1	64
Kero-Diesel gap (°C)*	−5–10	16.2	2.6	−0.9

* Standard practice

power generation, it also increases hydrogen and oxygen consumption, both of which ultimately convert into water.

In all three configurations, the required oxygen is obtained from the electrolyzer used to supply hydrogen to the plant. Power consumption is higher in Alternatives 1 and 2 compared to the original configuration, primarily due to the increased gas load in the FT compression section. Cooling demands are also greater in Alternatives 1 and 2, associated mainly with the condensers of the amine absorption unit's regenerator column and the steam turbine system.

In light of these findings, some broader conclusions can be drawn:

- SAF production capacity: Taking Spain as a reference, with an annual kerosene consumption of approximately 6600 kt/year [45], about 30 plants of the size studied in this work (225 kt/year) would be required to fully meet national demand.
- Hydrogen consumption: Producing 225 kt/year of SAF through the indirect CO_2-to-SAF route requires around 26,000 kg/h of hydrogen. Assuming that water electrolysis requires approximately 50 kWh/kg H_2 [46], a 1300 MWe power plant would be needed to generate the necessary electricity for hydrogen production alone. If this electricity were to come from solar power, and assuming a solar energy density of 50 W/m^2 [47], a solar plant covering roughly 26.3 km^2 would be needed, equivalent to 8.4 % of Spain's currently installed solar capacity [48]. Thus, even the entire existing solar infrastructure would not be sufficient to power the hydrogen production required to meet Spain's kerosene demand via this route.
- Alternative selection: The preferred process configuration should be selected based on whether the goal is to minimize electricity or hydrogen consumption. Alternative 1 has the lowest electricity demand, requiring 558 kWh per ton of product less than the original process, and 1165 kWh per ton less than Alternative 2. However, it consumes approximately 100 kg more hydrogen per ton of product compared to the other configurations. Based on a hydrogen price of 4.5 €/kg [49] and an electricity price of 80 €/MWh [25], the annual economic impact for a plant of this scale translates to savings of 18 million of euros in electricity if Alternative 1 is selected, or 174 million of euros in hydrogen if Alternative 2 is chosen (compared in both cases to the original alternative). Therefore, for a plant of this size, minimizing hydrogen consumption appears to be the more economically favorable strategy, considering that other parameters, such as land use and critical material demand, are expected to be similar in both cases due to the comparable number and size of the equipment. Moreover, considering that the RWGS and ATR reactors should ideally be integrated into a single furnace-type reactor to enhance heat recovery, Alternative 1 offers no real advantage in terms of equipment savings. In fact, it may result in higher capital expenditures due to the inclusion of a steam turbine. In a future scenario with much lower hydrogen production costs, a hybrid design approach between Alternatives 1 and 2, incorporating both an ATR reactor and a steam turbine, could be considered. This would balance hydrogen efficiency and electricity savings, although it may involve higher CAPEX. Lastly, the choice between an amine absorption unit or a PSA system to recover unreacted CO_2 from the RWGS reactor should be based on plant scale and specific equipment costs. Since the process is thermally self-sufficient, the reboiler duty of the regenerator column is not a significant concern. However, if a PSA is used, both CO_2 purity and recovery rate must be considered, as these factors directly impact overall product yields.
- Integration into an existing refinery or chemical plant: The integration of a CO_2-to-SAF production unit into an existing refinery or chemical plant would likely require the installation of a new CO_2 capture unit, using primarily flue gases from the facility's heaters as feedstock. The additional hydrogen needed could be supplied either by revamping an existing steam methane reforming unit, leveraging the new CO_2 capture unit for CO_2 recovery, or by installing electrolyzers. Some new intermediate and final storage tanks may also be required, along with revamping or installing units to provide the necessary utilities and flaring systems. The operation of the new SAF-production unit is not expected to interfere with the rest of the facility. However, planned or unplanned shutdowns could impact the SAF-production unit, since some of its feedstock and utilities are sourced from the facility.
- Minimum selling price of SAF: a preliminary economic analysis has been performed to determine the minimum selling price of SAF and to assess its sensitivity to key process variables such as the hydrogen production cost, the electricity price, the diesel selling price, and the CAPEX. The base-case scenario (detailed in the Supplementary

Material of this work) assumes a hydrogen production cost of 4.5 €/kg, an electricity price of 80 €/MWh, a diesel selling price of 0.75 €/L, and a CAPEX of 88.3 MM€. The minimum selling price, calculated to achieve a Net Present Value (NPV) of zero after ten years of operation, is 3.65 €/L. This is consistent with the IATA "Net Zero CO_2 Emissions Roadmap" [50], which estimates a minimum selling price of 3.77 €/L. However, this value is nearly five times higher than the minimum selling price of HEFA-derived SAF (0.78 €/L) and almost three times higher than that of alcohol-to-jet SAF (1.29 €/L) reported in the same roadmap. As shown in Fig. 2, the minimum selling price of SAF is most sensitive to the hydrogen production cost, followed by the diesel selling price, with electricity cost and CAPEX having a comparatively minor effect. These findings reveal that hydrogen cost is the dominant factor affecting SAF price, and therefore, efforts to reduce it through R&D should be prioritized. For example, reaching a minimum selling price of 0.65 €/L, comparable to current Jet A-1 market prices, would require approximately a tenfold reduction in hydrogen production cost, down to 0.45 €/kg.

5.3. Energy analysis

Heat integration is a key aspect in the design of sustainable processes aimed at producing net-zero fuels. To truly qualify as sustainable, a fuel must be synthesized in a process that minimizes CO_2 emissions, in line with the net-zero objective. These emissions are primarily associated with heating requirements, as heat generation typically relies on external fuel sources. For this reason, both Alternative 1 and Alternative 2 have been designed to be thermally self-sufficient, meaning that they operate without requiring any external heat input. A major challenge in the indirect CO_2-to-fuel route is the inclusion of the RWGS reactor, which operates at temperatures close to 900ºC. Two strategies are considered to supply this high temperature heat: using a dedicated furnace, as in Alternative 1, or integrating the ATR with the RWGS reactor, as in Alternative 2. Additionally, the use of a CO_2 capture unit via amine absorption introduces an extra heat demand that must be addressed. Fig. 3 presents the Sankey diagrams for both alternatives. To enhance clarity, minor streams have been omitted. The complete energy balances for both cases are available in the Supplementary Material of this work. As shown, both processes are thermally self-sufficient, requiring no external heat input. A significant portion of the heat content of the feed streams is released as waste heat: 53 % in Alternative 1 and 70 % in Alternative 2, primarily in the amine absorption unit, the Fischer-Tropsch unit, and the RWGS unit. In Alternative 1, a larger amount of heat is generated in the fired heater compared to the ATR in Alternative 2. This heat is recovered more effectively within the process, which results in a lower proportion of waste heat in Alternative 1.

If useful heat is defined as the combined heat content of the products and the heat supplied to the steam turbine, and supplied heat as the heat content of the feed streams plus compressors power, the resulting first-law efficiencies are 36 % for Alternative 1 and 30 % for Alternative 2. These results indicate that Alternative 1 achieves better overall energy utilization at the expense of higher hydrogen consumption.

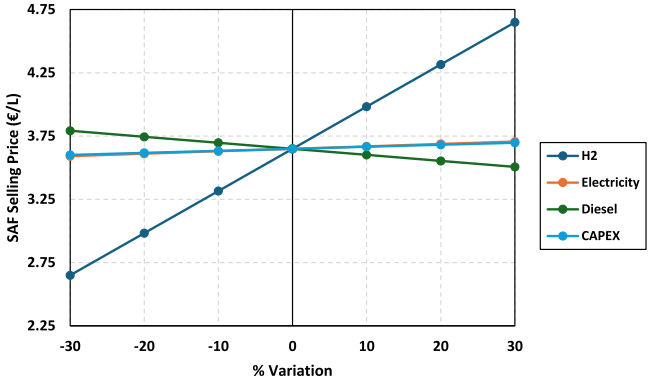

Fig. 2. Minimum selling price of SAF: sensitivity analysis.

After analyzing the energy balances, the results of the heat integration analysis conducted using pinch methodology are presented for both alternatives. The corresponding heat integration schemes and further integration opportunities are also discussed.

As shown in Fig. 4 and Fig. 5, both Alternative 1 and Alternative 2 achieve thermal self-sufficiency. However, several differences arise between the two configurations:

- The maximum temperature reached in Alternative 1 is significantly higher than in Alternative 2 due to the incorporation of a furnace. In contrast, the maximum temperature in Alternative 2 is limited to 950ºC, which corresponds to the operating temperature of the ATR. As previously discussed, the RWGS and ATR should ideally be integrated into a single furnace-type reactor to minimize thermal losses.
- In Alternative 2, a quasi-pinch occurs around 900ºC (Fig. 5), as all the heat generated in the ATR is utilized by the RWGS reactor. As outlined in the previous section, the heat output of the ATR can be tuned by adjusting the O_2/C ratio. However, increasing oxygen input raises the duty but reduces hydrogen output. Therefore, the ATR in Alternative 2 has been adjusted to supply the amount of heat required by the RWGS reactor. In contrast, Alternative 1 does not present a pinch point, as the furnaces release an excess of heat. This surplus is used for generating steam at lower temperatures.
- Cooling requirements are notably higher in Alternative 1 (670 MW) than in Alternative 2 (429 MW). This difference is primarily due to the additional duty required for the condenser in the steam turbine system of Alternative 1.

From a design perspective, several important considerations must be taken into account:

- The duty required for the regenerator in the amine absorption unit is particularly high, being approximately 230–250 MW for a 225 kt/year SAF plant. This is considerably high when compared to other process units, such as the downstream distillation columns, which require only 2–10 MW. Therefore, it is essential to carefully optimize the design and operation of the regenerator column to reduce heat consumption while ensuring effective CO_2 capture. Most of the required heat is sourced from the FT reactor, which releases a significant amount of thermal energy in the same range as the one consumed in the regenerator reboiler.
- The reboiler of the DWC operates at temperatures between 240–260ºC, needing high pressure steam (approximately at 50–60 bar). This steam can be produced using high temperature sources such as the RWGS furnace in Alternative 1 or the hot product stream from the ATR in Alternative 2. The same requirement applies to the reboilers in both the stripper & distillation column configuration and the distillation column with pumparound and lateral stripper configuration.
- Both alternatives exhibit an excess of heat in the 150–200ºC temperature range. This surplus of thermal energy can be utilized to produce low or medium-pressure steam, which may be exported to other units or external facilities. The main contributors to this excess are the product streams from the FT reactor and flue gases from the heaters in Alternative 1, and the product streams from the RWGS reactor, FT reactor, and ATR in Alternative 2.

5.4. Sustainability indicators

The environmental sustainability of the three alternatives analyzed in this work has been compared using a set of indicators commonly found in the literature [44,45]. Lower values of these indicators correspond to better performance from an environmental sustainability

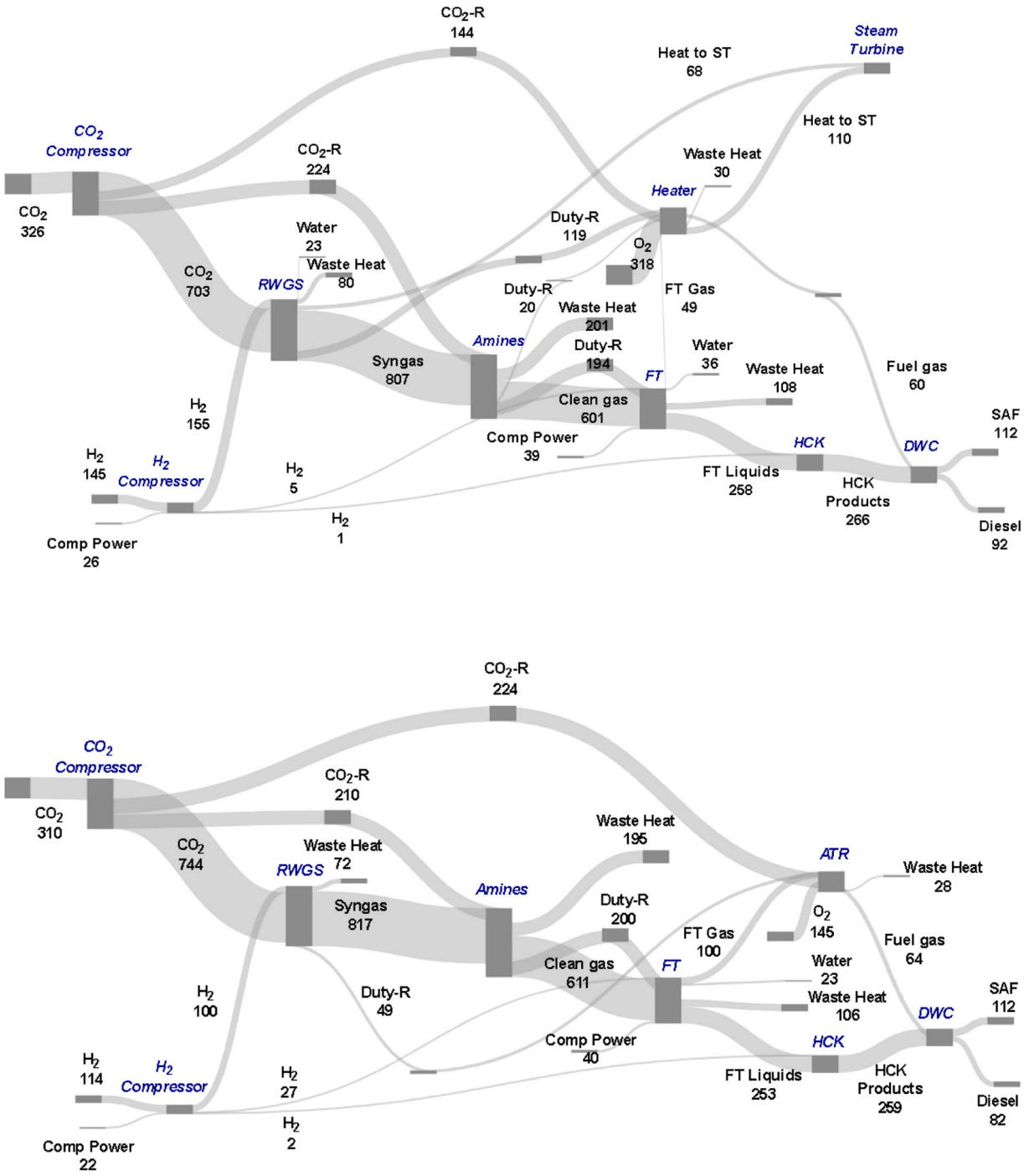

Fig. 3. Sankey diagrams (Gcal/h) for Alternatives 1 (upper) and 2 (lower).

perspective. Table 5 summarizes the values for all the metrics, which are discussed in detail below:

- Material intensity: This indicator represents the total amount of raw materials required to produce a unit of product. In the present process, the main raw materials are CO_2, hydrogen, and oxygen, while the two products are SAF and diesel. As shown in Table 5, Alternative 1 exhibits the highest material intensity (5.21 kg of raw materials per kg of products), followed by Alternative 2 (4.29 kg/kg) and the original process (4.14 kg/kg). This trend is primarily driven by the greater hydrogen and oxygen consumption in Alternatives 1 and 2, particularly in Alternative 1, where additional hydrogen and oxygen are consumed to generate the extra duty required in the RWGS and hydrocracker furnaces. One of the key advantages of producing SAF via the CO_2-to-FT route is the high drop-in compatibility of the resulting fuel, which can be blended with conventional Jet A-1 at ratios of up to 50 % [10]. Compared to conventional Jet A-1 production from petroleum, the FT route also offers the benefit of producing fuels with lower sulfur oxides (SOx) and nitrogen oxides (NOx) emissions, particularly when starting from relatively pure CO_2 streams. This eliminates the need for hydrotreating, thereby reducing the material intensity and complexity of the production plant.
- E-factor: This metric quantifies the mass of byproducts generated per kilogram of product. In this case, water is considered the main byproduct, produced during the CO_2 hydrogenation reactions. Given

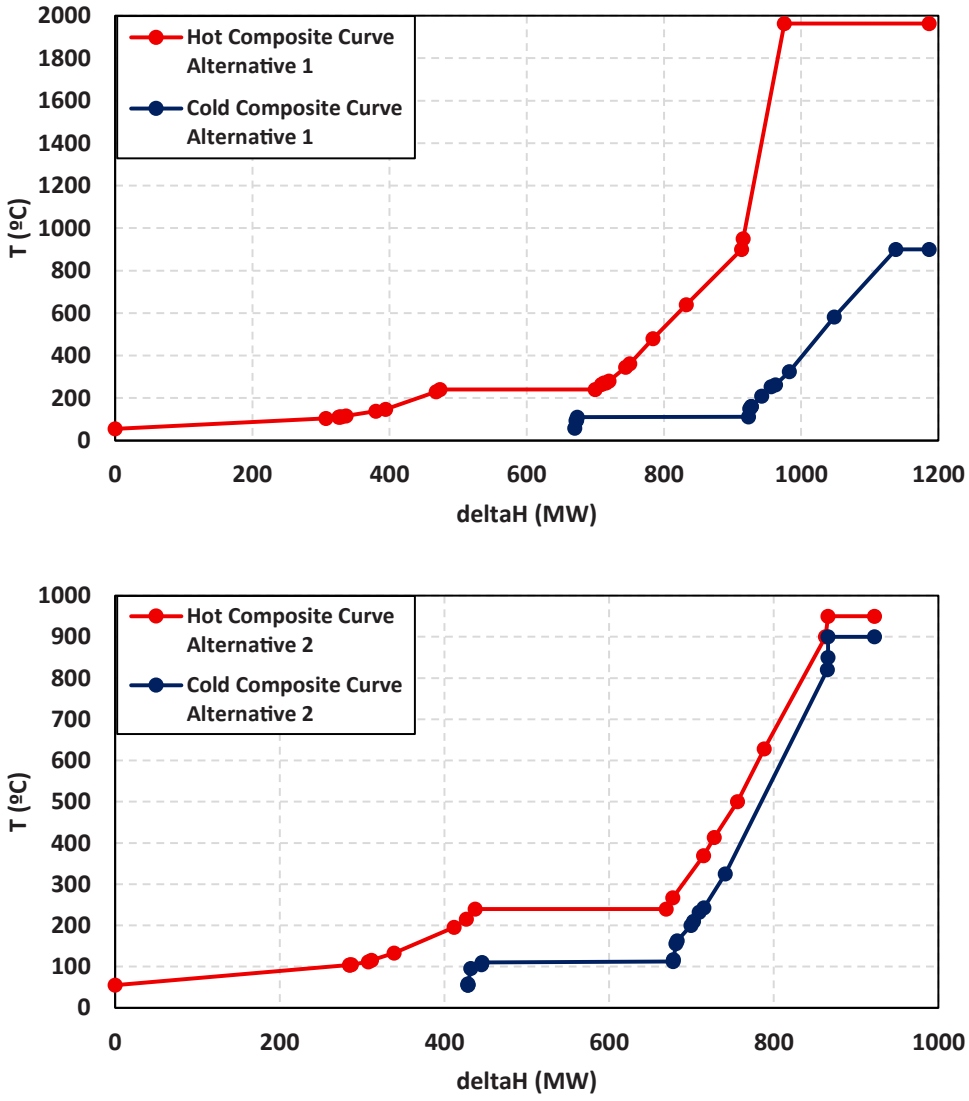

Fig. 4. Hot and cold composite curves for Alternatives 1 (upper) and 2 (lower).

the high purity of the recovered water, it could be used as makeup water for the cooling system to compensate for evaporation losses, although some preliminary treatments, such as degassing, would be necessary. As expected, Alternative 1 presents the highest E-factor (4.21 kg of water per kg of products), due to the larger amount of water formed in the combustion processes. It is followed by Alternative 2 (3.29 kg/kg) and the original process (3.14 kg/kg). This work assumes the use of pure CO_2 and wet hydrogen as feedstocks. While water present in the streams is expected to condense and be removed in the interstage knockout (KO) drums of the compressors, other potential impurities, such as nitrogen, sulfur compounds, or trace contaminants, pose a more significant risk, as these impurities can deactivate or poison the catalysts used throughout the plant. Therefore, a preconditioning step would be necessary to purify the feed gases, ensuring compatibility with catalyst requirements. However, such treatment would increase the E-factor of the process.

- Energy intensity: This indicator measures the amount of energy consumed per unit of product. Given that the processes are thermally self-sufficient, only the energy consumed by compressors is considered. The energy intensity results align with the net power consumption figures shown in Table 2. Alternative 2 shows the highest energy intensity (1.71 kWhe per kg of products), followed by the original alternative (1.53 kWhe/kg), while Alternative 1 has the lowest energy intensity (0.71 kWhe/kg), due to energy recovery via the implementation of a steam turbine. Intermittency in renewable electricity supply would affect process performance if no additional measures such as batteries, hydrogen storage facilities or alternative power and hydrogen sources are implemented. If grey electricity (produced from fossil fuels) is used instead of renewable electricity, and assuming a conversion factor of 2.5 units of primary energy per unit of electricity, the total energy requirements increase up to 4.28 kWhe/kg of product for Alternative 2, 3.83 kWhe/kg for the original configuration, and 1.78 kWhe/kg for Alternative 1. Upstream, the water electrolyzers used to generate hydrogen are assumed to consume approximately 50 kWhe/kgH_2 [46]. Based on this value, the total electricity requirement for hydrogen production ranges between 25 and 31 kWhe/kg of products (SAF and diesel). When primary energy is considered, this corresponds to 63–78 kWhe/kg of products.
- Water consumption: This metric indicates the amount of fresh water consumed per kilogram of products. Although the plant does not directly consume water as a reagent or utility, since air-cooled heat exchangers are used, this analysis assumes water-based cooling. Assuming a typical loss of 7 % in the cooling tower and a 10ºC temperature difference between the cooling water inlet and outlet, the estimated water consumption ranges from 0.02 m^3 /kg for the

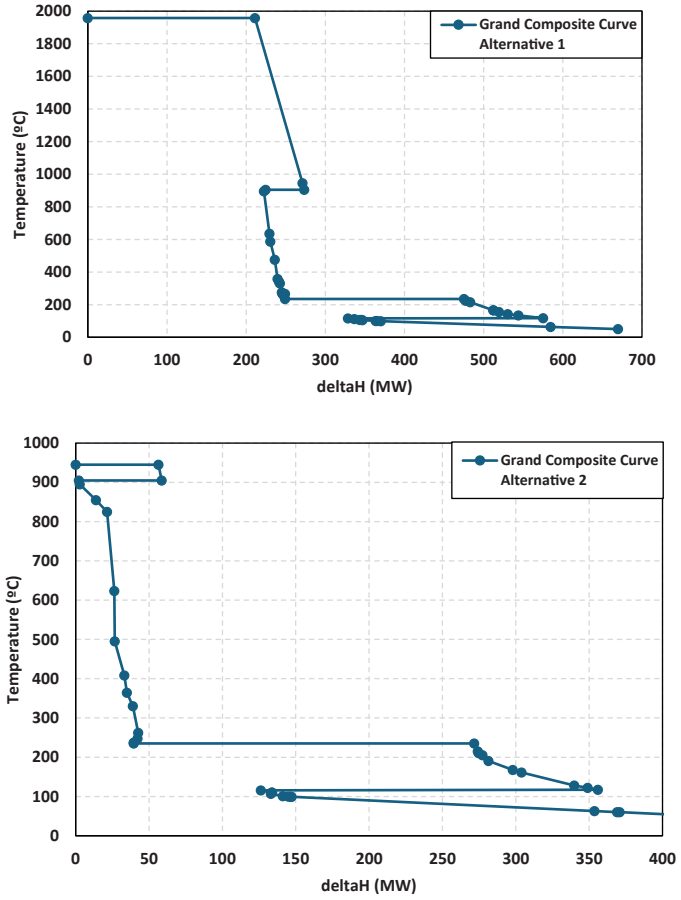

Fig. 5. Grand composite curves for Alternative 1 (upper) and 2 (lower).

Table 4
Separation alternatives: KPIs (upper table) and product specifications (lower table).

	Stripper + DC	DC+PA+Stripper	DWC
Light Gases yield (%)	23.8	23.8	23.8
SAF yield (%)	51.9	51.9	51.9
Diesel yield (%)	24.2	24.2	24.2
Reboiler Duty (kW)	703 + 5075	3460 + 271	2572
Condenser Duty (kW)	6375 + 4344	5990 + 2715 (PA)	7463
Number of trays	11 + 23	25 + 2	23

	Spec	Stripper + DC	DC+PA+Stripper	DWC
SAF				
Flash Point (ºC)	38, min	38	38	38
Freezing Point (ºC)	−47, max	−53	−53	−53
ASTM D86, 10 % v/v (ºC)	205, max	154	154	154
ASTM D86, FBP (ºC)	300, max	242	239	235.2
Density at 15ºC (kg/m^3)	730–770	763	759	760
Diesel				
Flash Point (ºC)	55, min	89	89	90
ASTM D86, 95 % v/v (ºC)	360, max	360	360	360
Density at 15ºC (kg/m^3)	845, max	785	787	787
Cetane number	51, min	68	68	69
Kero-Diesel gap (ºC)*	−5–10	1.2	3.3	3.7

*Standard practice

Table 5
Sustainability metrics for the proposed alternatives.

	Atsonios (2023)	This Work-No ATR	This Work-Optimized
Material Intensity (kgmat/kgprod)	4.14	5.21	4.29
E-Factor (kgbyprod/kgprod)	3.14	4.21	3.29
Energy Intensity (kWhe/kgprod)	1.53	0.71	1.71
Water Consumption (m^{3}water/kgprod)	0.02	0.07	0.05
GHG Emissions (kgCO_2eq/kgprod)	1.07	1.30	1.11

original process, to 0.07 m^3 /kg for Alternative 1, and up to 0.05 m^3 /kg for Alternative 2. The largest contributors to water demand are the condenser of the regenerator column in the amine absorption unit (Alternatives 1 and 2) and the condenser of the steam turbine (Alternative 1). The minimum temperature within the process has been fixed at 55 °C. This makes it possible to use air-cooled heat exchangers instead of trim-cooled ones, particularly beneficial in arid regions with limited access to water. However, this would result in increased electricity demand due to the power consumption of air coolers. If higher minimum temperatures are required, the plant could be redesigned with increased operating pressures and temperatures, though this would raise both CAPEX and OPEX. In terms of water demand, hydrogen production via electrolysis has a theoretical water consumption of approximately 9 kgH_2O/kgH_2. This corresponds to a minimum additional water requirement of

approximately 0.006 m^3H_2O/kg of products in all three process alternatives considered.

- Greenhouse gas GHG emissions: This parameter accounts for the GHG emissions expressed in $kgCO_2eq$ per kilogram of products. Since all alternatives operate using green electricity and are thermally self-sufficient, the emissions in the production plant are associated with hydrogen production, CO_2 capture, and electricity generation. Among the alternatives, Alternative 1 shows the highest GHG emissions (1.3 $kgCO_2eq$/kg of products), followed by Alternative 2 (1.11 $kgCO_2eq$/kg of products) and the original process (1.07 $kgCO_2eq$/kg of products). This trend mirrors the hydrogen consumption pattern, which is the dominant contributor to GHG emissions. As in previous works [25,26], the GHG emissions are calculated assuming that the electricity is produced from wind power. If the CO_2 consumed in the process is taken into account, the net GHG emissions of the production plant become negative and in the range of −2 $kgCO_2eq$/kg of products for the original process and Alternative 2, and −1.8 $kgCO_2eq$/kg of products for Alternative 1. If grey electricity (produced from natural gas) and grey hydrogen (produced by steam reforming of methane without carbon capture) are used, the GHG emissions increase up to 5.58 $kgCO_2eq$/kg of products in Alternative 1, 5.21 $kgCO_2eq$/kg of products in Alternative 2, and 5 $kgCO_2eq$/kg of products in the original process. If CO_2 consumption is accounted for, the net GHG emissions are in the range of 2 $kgCO_2eq$/kg of products for the original process and Alternative 2, and 2.5 $kgCO_2eq$/kg of products for Alternative 1.

When compared with our previous studies on the sustainable production of chemicals and fuels, such as methanol and DME, via CO_2 hydrogenation [25,26], and taking Alternative 2 as a baseline, the process analyzed here shows higher material and energy intensities, greater water consumption, and increased GHG emissions. The indirect CO_2-to-SAF route involves three separate reactors that consume hydrogen (RWGS, FT, and hydrocracker). Additionally, unlike previous processes, the outlet stream from the amine absorption unit must be compressed again to 35 bar. The higher thermal output of the process also leads to significant cooling requirements, although some of the excess heat can be used for steam generation and export. Finally, the higher overall hydrogen demand leads to increased GHG emissions. However, when taking into account the CO_2 consumed as reagent, the net emissions are lower than those reported for our previous processes.

6. Conclusions

This work has presented and compared three thermally self-sufficient alternatives for the production of sustainable aviation fuel (SAF) via indirect CO_2 hydrogenation. The first configuration corresponds to the original process developed by Atsonios et al. (2023) [7], which is based on a combination of RWGS, FT, hydrocracker, and ATR reactors. The first alternative replaces the ATR with two furnaces and incorporates a CO_2 capture unit based on amine absorption, an isomerization bed, a Dividing Wall Column (DWC), and a steam turbine. The second alternative retains the ATR while also including the CO_2 capture unit, the isomerization bed, and the DWC. The main findings of this work are summarized below:

- A commercial-scale plant with a production capacity of 225 ktpy can supply approximately 3.4 % of Spain's annual kerosene demand. This requires about 26,000 kg/h of green hydrogen, corresponding to approximately 1300 MWe of installed power capacity, or around 8.4 % of Spain's current solar power infrastructure.
- At this scale, minimizing hydrogen consumption (Alternative 2) is economically more favorable than reducing electricity usage (Alternative 1), due to the high cost of hydrogen production via electrolysis. Assuming a hydrogen production cost of 4.5 €/kg and an electricity price of 80 €/MWh results in a minimum selling price of SAF of 3.65 €/L, about six times higher than the current production cost of Jet A-1 (0.65 €/L). Achieving price parity with Jet A-1 would require approximately a tenfold reduction in hydrogen production cost. In this context, carbon credits and energy subsidies are expected to favor Alternative 2, given its greater GHG emissions reduction and higher renewable electricity consumption. Furthermore, integrating the RWGS and ATR reactors into a single furnace-type unit is recommended to enhance heat integration and reduce capital costs. The inclusion of an isomerization reactor or bed after the hydrocracker is essential to produce branched paraffins and meet the freezing point requirements of SAF. Finally, the decision between using an amine absorption unit or a PSA system will depend on equipment cost and the CO_2 recovery rate of the PSA, since the heat required for the amine regenerator can be supplied by steam generated within the SAF plant.
- The use of a Dividing Wall Column (DWC) is advantageous compared to either a combination of a stripper and distillation column or a single column with pumparound and lateral stripper. The DWC requires fewer trays (23) and a lower reboiler duty (2572 kW). Furthermore, as raw material variability is not expected, operational flexibility is not a concern, which minimizes potential controllability issues.
- From an environmental perspective, all process alternatives only generate water as a byproduct and achieve negative greenhouse gas (GHG) emissions in the range of −2 kg CO_2eq per kg of product. These emissions are primarily associated with CO_2 capture and the production of hydrogen and electricity. However, the substantial hydrogen consumption across the RWGS, FT, and hydrocracker reactors results in a relatively high material intensity (4.2–5.2 kg of raw materials per kg of product), especially when compared with previous processes for the sustainable production of chemicals such as methanol and DME.

Funding

This research did not receive any specific grant from funding agencies in the public, commercial, or not-for-profit sectors.

CRediT authorship contribution statement

Diego Rego-Fernández: Writing – original draft, Investigation. **Luis Vaquerizo:** Writing – review & editing, Writing – original draft, Validation, Supervision, Project administration, Methodology, Investigation, Formal analysis, Conceptualization.

Declaration of Competing interest

The authors declare that they have no known competing financial interests or personal relationships that could have appeared to influence the work reported in this paper.

Acknowledgments

The authors thank María Ibáñez Pardo, MSc in Chemical Engineering, for her contributions to the simulation of the original process proposed by Atsonios et al. (2023) [7].

Appendix A. Supporting information

Supplementary data associated with this article can be found in the online version at doi:10.1016/j.jcou.2025.103225.

Data availability

No data was used for the research described in the article.

References

[1] C. Bergero, G. Gosnell, D. Gielen, S. Kang, M. Bazilian, S.J. Davis, Pathways to net-zero emissions from aviation, Nat. Sustain 6 (2023) 404–414, https://doi.org/10.1038/s41893-022-01046-9.

[2] S. Bube, N. Bullerdiek, S. Voß, M. Kaltschmitt, Kerosene production from power-based syngas – a technical comparison of the Fischer-Tropsch and methanol pathway, Fuel 366 (2024) 131269, https://doi.org/10.1016/j.fuel.2024.131269.

[3] V. Grewe, A. Gangoli Rao, T. Grönstedt, C. Xisto, F. Linke, J. Melkert, J. Middel, B. Ohlenforst, S. Blakey, S. Christie, S. Matthes, K. Dahlmann, Evaluating the climate impact of aviation emission scenarios towards the Paris agreement including COVID-19 effects, Nat. Commun. 12 (2021) 1–10, https://doi.org/10.1038/s41467-021-24091-y.

[4] International Air Transport Association (IATA), Net zero carbon 2050 resolution, 2021. ⟨https://www.iata.org/en/iata-repository/pressroom/fact-sheets/fact-sheet-iata-net-zero-resolution/⟩ (accessed June 12, 2025).

[5] A. Gonzalez-Garay, C. Heuberger-Austin, X. Fu, M. Klokkenburg, D. Zhang, A. van der Made, N. Shah, Unravelling the potential of sustainable aviation fuels to decarbonise the aviation sector, Energy Environ. Sci. 15 (2022) 3291–3309, https://doi.org/10.1039/d1ee03437e.

[6] S. Bube, S. Voß, G. Quante, M. Kaltschmitt, Cost analysis of kerosene production from power-based syngas via the Fischer-Tropsch and methanol pathway, Fuel 384 (2025) 133901, https://doi.org/10.1016/j.fuel.2024.133901.

[7] K. Atsonios, J. Li, V.J. Inglezakis, Process analysis and comparative assessment of advanced thermochemical pathways for e-kerosene production, Energy 278 (2023) 127868, https://doi.org/10.1016/j.energy.2023.127868.

[8] G. Quante, N. Bullerdiek, S. Bube, U. Neuling, M. Kaltschmitt, Renewable fuel options for aviation – a System-Wide comparison of Drop-In and non Drop-In fuel options, Fuel 333 (2023) 126269, https://doi.org/10.1016/j.fuel.2022.126269.

[9] M. Wang, R. Dewil, K. Maniatis, J. Wheeldon, T. Tan, J. Baeyens, Y. Fang, Biomass-derived aviation fuels: challenges and perspective, Prog. Energy Combust. Sci. 74 (2019) 31–49, https://doi.org/10.1016/j.pecs.2019.04.004.

[10] M.F. Shahriar, A. Khanal, The current techno-economic, environmental, policy status and perspectives of sustainable aviation fuel (SAF), Fuel 325 (2022) 124905, https://doi.org/10.1016/j.fuel.2022.124905.

[11] M. Marchese, E. Giglio, M. Santarelli, A. Lanzini, Energy performance of Power-to-Liquid applications integrating biogas upgrading, reverse water gas shift, solid oxide electrolysis and Fischer-Tropsch technologies, Energy Convers. Manag. X 6 (2020) 100041, https://doi.org/10.1016/j.ecmx.2020.100041.

[12] C. Panzone, R. Philippe, A. Chappaz, P. Fongarland, A. Bengaouer, Power-to-Liquid catalytic CO2 valorization into fuels and chemicals: focus on the Fischer-Tropsch route, J. CO2 Util. 38 (2020) 314–347, https://doi.org/10.1016/j.jcou.2020.02.009.

[13] Y. Han, A.D.N. Kamkeng, O. Otitoju, Y. Ding, M. Wang, Techno-economic assessment of modified Fischer-Tropsch synthesis process for direct CO2 conversion into jet fuel, Fuel 381 (2025) 133442, https://doi.org/10.1016/j.fuel.2024.133442.

[14] A.D.N. Kamkeng, M. Wang, Technical analysis of the modified Fischer-Tropsch synthesis process for direct CO2 conversion into gasoline fuel: performance improvement via ex-situ water removal, Chem. Eng. J. 462 (2023) 142048, https://doi.org/10.1016/j.cej.2023.142048.

[15] B. Yao, T. Xiao, O.A. Makgae, X. Jie, S. Gonzalez-Cortes, S. Guan, A.I. Kirkland, J. R. Dilworth, H.A. Al-Megren, S.M. Alshihri, P.J. Dobson, G.P. Owen, J.M. Thomas, P.P. Edwards, Transforming carbon dioxide into jet fuel using an organic combustion-synthesized Fe-Mn-K catalyst, Nat. Commun. 11 (2020) 1–12, https://doi.org/10.1038/s41467-020-20214-z.

[16] L. Zhang, Y. Dang, X. Zhou, P. Gao, A. Petrus van Bavel, H. Wang, S. Li, L. Shi, Y. Yang, E.I. Vovk, Y. Gao, Y. Sun, Direct conversion of CO2 to a jet fuel over CoFe alloy catalysts, Innovation 2 (2021) 1–9, https://doi.org/10.1016/j.xinn.2021.100170.

[17] P. Hirunsit, A. Senocrate, C.E. Gómez-Camacho, F. Kiefer, From CO2 to sustainable aviation fuel: navigating the technology landscape, ACS Sustain Chem. Eng. 12 (2024) 12143–12160, https://doi.org/10.1021/acssuschemeng.4c03939.

[18] S. Pratschner, M. Hammerschmid, S. Müller, F. Winter, Evaluation of CO2 sources for Power-to-Liquid plants producing Fischer-Tropsch products, J. CO2 Util. 72 (2023) 102508, https://doi.org/10.1016/j.jcou.2023.102508.

[19] D.H. König, N. Baucks, R.U. Dietrich, A. Wörner, Simulation and evaluation of a process concept for the generation of synthetic fuel from CO2 and H2, Energy 91 (2015) 833–841, https://doi.org/10.1016/j.energy.2015.08.099.

[20] J. Baltrusaitis, W.L. Luyben, Methane conversion to syngas for Gas-to-Liquids (GTL): is sustainable CO2 reuse via dry methane reforming (DMR) cost competitive with SMR and ATR processes? ACS Sustain Chem. Eng. 3 (2015) 2100–2111, https://doi.org/10.1021/acssuschemeng.5b00368.

[21] Z. Navas-Anguita, P.L. Cruz, M. Martín-Gamboa, D. Iribarren, J. Dufour, Simulation and life cycle assessment of synthetic fuels produced via biogas dry reforming and Fischer-Tropsch synthesis, Fuel 235 (2019) 1492–1500, https://doi.org/10.1016/j.fuel.2018.08.147.

[22] M. Panahi, A. Rafiee, S. Skogestad, M. Hillestad, A natural gas to liquids process model for optimal operation, Ind. Eng. Chem. Res. 51 (2012) 425–433, https://doi.org/10.1021/ie2014058.

[23] Y. Liu, K. Murata, K. Okabe, M. Inaba, I. Takahara, T. Hanaoka, K. Sakanishi, Selective hydrocracking of fischer-tropsch waxes to high-quality diesel fuel over pt-promoted polyoxocation-pillared montmorillonites, Top. Catal. 52 (2009) 597–608, https://doi.org/10.1007/s11244-009-9239-8.

[24] A. Meurer, J. Kern, Fischer–tropsch synthesis as the key for decentralized sustainable kerosene production, Energies 14 (2021) 1–21, https://doi.org/10.3390/en14071836.

[25] L. Vaquerizo, A.A. Kiss, Thermally self-sufficient process for cleaner production of e-methanol by CO2 hydrogenation, J. Clean. Prod. 433 (2023) 139845, https://doi.org/10.1016/j.jclepro.2023.139845.

[26] L. Vaquerizo, A.A. Kiss, Thermally self-sufficient process for single-step coproduction of methanol and dimethyl ether by CO2hydrogenation, J. Clean. Prod. 441 (2024) 140949, https://doi.org/10.1016/j.jclepro.2024.140949.

[27] Boeing, Boeing 737, (2007). ⟨https://www.boeing.com/content/dam/boeing/boeingdotcom/company/about_bca/startup/pdf/historical/737NG_passenger.pdf⟩ (accessed July 3, 2025).

[28] AENA, Tráfico de pasajeros, operaciones y carga en la red de AENA, (2024). file:///C:/Users/usuario/Downloads/Informe+Provisional+Anual+2024.pdf (accessed July 3, 2025).

[29] R.M. El-Maghraby, A study on bio-diesel and jet fuel blending for the production of renewable aviation fuel. in: Materials Science Forum, Trans Tech Publications Ltd, 2020, pp. 231–244, https://doi.org/10.4028/www.scientific.net/MSF.1008.231.

[30] T.A. Adams, P.I. Barton, Combining coal gasification and natural gas reforming for efficient polygeneration, Fuel Process. Technol. 92 (2011) 639–655, https://doi.org/10.1016/j.fuproc.2010.11.023.

[31] H. Jahangiri, J. Bennett, P. Mahjoubi, K. Wilson, S. Gu, A review of advanced catalyst development for Fischer-Tropsch synthesis of hydrocarbons from biomass derived syn-gas, Catal. Sci. Technol. 4 (2014) 2210–2229, https://doi.org/10.1039/c4cy00327f.

[32] A.P. Savost'yanov, O.L. Eliseev, R.E. Yakovenko, G.B. Narochniy, K.I. Maslakov, I. Zubkov, V.N. Soromotin, A.T. Kozakov, A.V. Nicolskii, S.A. Mitchenko, Deactivation of Co-Al2O3/SiO2 Fischer–Trospch synthesis catalyst in industrially relevant conditions, Catal. Lett. 150 (2020) 1932–1941, https://doi.org/10.1007/s10562-020-03097-z.

[33] M.R. Rahimpour, H. Elekaei, A comparative study of combination of Fischer-Tropsch synthesis reactors with hydrogen-permselective membrane in GTL technology, Fuel Process. Technol. 90 (2009) 747–761, https://doi.org/10.1016/j.fuproc.2009.02.011.

[34] N. Jurtz, G.D. Wehinger, U. Srivastava, T. Henkel, M. Kraume, Validation of pressure drop prediction and bed generation of fixed-beds with complex particle shapes using discrete element method and computational fluid dynamics, AIChE J. 66 (2020) 1–13, https://doi.org/10.1002/aic.16967.

[35] A. Sari, Y. Zamani, S.A. Taheri, Intrinsic kinetics of Fischer-Tropsch reactions over an industrial Co-Ru/γ-Al2O3 catalyst in slurry phase reactor, Fuel Process. Technol. 90 (2009) 1305–1313, https://doi.org/10.1016/j.fuproc.2009.06.024.

[36] T. Riedel, G. Schaub, Low-temperature Fischer-Tropsch synthesis on cobalt catalysts-effects of CO2, Top. Catal. 26 (2003) 145–156, https://doi.org/10.1023/B:TOCA.0000012995.42657.ca.

[37] S. Gamba, L.A. Pellegrini, V. Calemma, C. Gambaro, Liquid fuels from Fischer-Tropsch wax hydrocracking: isomer distribution, Catal. Today 156 (2010) 58–64, https://doi.org/10.1016/j.cattod.2010.01.009.

[38] Koch-Glitsch, Flexipac H.C., (2025). ⟨https://www.koch-glitsch.com/product-catalog?product=flexipac-hc-structured-packing⟩ (accessed June 26, 2025).

[39] T. Giampaolo, Compressor handbook principles and practices, The Fairmont Press, 2010.

[40] Gas Processors Suppliers Association, GPSA Engineering Data Book, Twelfth Edition, Gas Processors Suppliers Association, Oklahoma, 2004.

[41] E. Rytter, M. Hillestad, R. Lovstad, B.Oyvind Bringedal, Prod. Hydrocarb. (2021).

[42] Siemens, Siemens Steam Turbines, (2025). ⟨https://www.siemens-energy.com/global/en/home/products-services/product/industrial-steam-turbines.html#Technical-Data-and-Typical-Applications-tab-9⟩ (accessed July 2, 2025).

[43] A. Raimondi, A. Favela-Contreras, F. Beltrán-Carbajal, A. Piñón-Rubio, J. Luis de la Peña-Elizondo, Design of an adaptive predictive control strategy for crude oil atmospheric distillation process, Control Eng. Pr. 34 (2015) 39–48, https://doi.org/10.1016/j.conengprac.2014.09.014.

[44] Ö. Yildirim, A.A. Kiss, E.Y. Kenig, Dividing wall columns in chemical process industry: a review on current activities, Sep Purif. Technol. 80 (2011) 403–417, https://doi.org/10.1016/j.seppur.2011.05.009.

[45] Comisión Nacional de los Mercados y la Competencia (CNMC), Estadística de productos petrolíferos, (2024). ⟨https://www.cnmc.es/estadistica/estadistica-de-productos-petroliferos⟩ (accessed July 3, 2025).

[46] M. Wanner, Transformation of electrical energy into hydrogen and its storage, Eur. Phys. J. 136 (2021), https://doi.org/10.1140/epjp/s13360-021-01585-8.

[47] B. Shiva Kumar, K. Sudhakar, Performance evaluation of 10 MW grid connected solar photovoltaic power plant in India, Energy Rep. 1 (2015) 184–192, https://doi.org/10.1016/j.egyr.2015.10.001.

[48] P. y Alimentación.G. de E. Ministerio de Agricultura, Extensión de los parques fotovoltaicos en España, 2024. ⟨https://www.mapa.gob.es/dam/mapa/contenido/ministerio/servicios/servicios-de-informacion/analisis-y-prospectiva/ayp-serie-agrinfo/ayp_37_parquefotovoltaico.pdf⟩ (accessed July 3, 2025).

[49] S. Shiva Kumar, H. Lim, An overview of water electrolysis technologies for Green hydrogen production, Energy Rep. 8 (2022) 13793–13813, https://doi.org/10.1016/j.egyr.2022.10.127.

[50] International Air Transport Association (IATA), Finance Net Zero CO2 Emissions Roadmap, 2024. ⟨https://www.iata.org/contentassets/8d19e716636a47c184e7221c77563c93/finance-net-zero-roadmap.pdf⟩ (accessed September 3, 2025).